

Decay properties of the neutron-rich isotopes,  $^{11}\text{Li}$  and  $^{27-31}\text{Na}$ 

E. Roeckl,\* P. F. Dittner,† C. Détraz,‡ R. Klapisch, C. Thibault, and C. Rigaud  
*Laboratoire René-Bernas du Centre de Spectrométrie Nucléaire et de Spectrométrie de Masse,  
 91406 Orsay, France*

(Received 28 May 1974)

Using an on-line mass spectrometer the decay properties of the  $T_z \geq \frac{5}{2}$  nuclei  $^{11}\text{Li}$ ,  $^{27-31}\text{Na}$ ,  $^{29,30}\text{Mg}$  were studied. The new isotope  $^{30}\text{Mg}$  ( $T_{1/2} = 1200 \pm 500$  msec) was identified by  $\beta$  counting. For the other isotopes the half-lives were remeasured by three independent methods with improved precision. By recording  $\beta$ -coincident  $\gamma$  spectra, the decays of  $^{27-29}\text{Na}$  were studied, leading to a  $1^+$  assignment for the  $^{28}\text{Na}$  ground state. By simultaneous  $\beta$  and neutron multiscaling the delayed neutron emission probabilities  $P_n$  were determined for  $^{11}\text{Li}$  and  $^{27-31}\text{Na}$ . The following half-lives (msec) and  $P_n$  values (%) were found (errors see text):  $^{11}\text{Li}$  (8.5/60.8),  $^{27}\text{Na}$  (304/0.08),  $^{28}\text{Na}$  (30.5/0.58),  $^{29}\text{Na}$  (42.9/15.1),  $^{30}\text{Na}$  (53.0/33.1),  $^{31}\text{Na}$  (16.9/30).

RADIOACTIVITY  $^{9,11}\text{Li}$ ,  $^{27,28,29,30,31}\text{Na}$ ,  $^{29,30}\text{Mg}$ ; measured  $T_{1/2}$ ,  $E_\beta$ ,  $\beta\gamma$  coin, delayed neutrons; deduced  $E_\gamma$ ,  $I_\gamma$ ,  $\log ft$ ,  $Q$ ,  $J$ ,  $\pi$ ,  $P_n$ . On-line mass separation.

## 1. INTRODUCTION

Very neutron-rich, low- $Z$  isotopes have recently been produced with high-energy protons<sup>1,2</sup> or by heavy-ion-induced transfer reactions.<sup>3</sup> The methods applied for the identification of these isotopes were either on-line mass spectrometry<sup>4,5</sup> or the particle identification technique combined with time-of-flight<sup>6</sup> or magnetic analysis.<sup>7,8</sup>

By the particle identification technique a large number of new isotopes have been found<sup>9</sup> and in a few cases their ground state masses have been measured.<sup>10</sup> Using on-line mass separation, on the other hand, not only the identification<sup>2</sup> of ground states and the determination of their masses (measured directly<sup>11,12</sup> or via the  $Q_\beta$  value of the  $\beta$  decay<sup>13</sup>) becomes possible, but also the investigation of  $\beta$  decay and of subsequent decay phenomena. Thereby information about the nuclear properties of states involved in the  $\beta$  decay of nuclei with a large excess of neutrons can be gained.

Whereas successful mass measurements have been performed recently for  $T_z = \frac{5}{2}$  nuclei in the  $2s-1d$  shell (for a compilation see Ref. 14), very little spectroscopic information exists for nuclei with  $T_z \geq \frac{5}{2}$ . In this paper, we report<sup>15</sup> on a study of  $\beta$  delayed neutron and  $\gamma$  emission from the isotopes  $^{11}\text{Li}$  ( $T_z = \frac{5}{2}$ ),  $^{27-31}\text{Na}$  ( $T_z = \frac{5}{2} - \frac{3}{2}$ ), and  $^{29,30}\text{Mg}$  ( $T_z = \frac{5}{2}$ , 3).

## 2. EXPERIMENTAL

## A. Isotope production

Details of the on-line spectrometer have already been described elsewhere.<sup>4,5</sup> Essentially, the en-

ergetic recoils from the reaction of 24 GeV protons from the CERN proton synchrotron with uranium are caught in heated graphite, from which alkali elements diffuse very quickly. Ions produced by surface ionization are accelerated and analyzed in a magnetic prism. The mass separated ion beam is refocused by two triplets of electrostatic quadrupole lenses on an electron multiplier located in a well shielded area several meters away from the proton beam. For spectroscopy measurements the multiplier was replaced by a thin stainless steel catcher in front of which different detectors could be located.

The target is bombarded with short (2.1  $\mu\text{sec}$ ) proton bursts of about  $1.5 \times 10^{12}$  protons every 10 sec. The growth and decay of activity collected on the catcher after the burst is governed by the diffusion characteristics and by the half-life of the isotope in question. The ion beam can be switched off by a fast electrostatic deflector after a suitable collection time, in order to get the pure radioactive decay undisturbed by diffusion.

## B. Delayed neutron detection

The neutron detector<sup>16</sup> consisted of eight  $^3\text{He}$  proportional counters embedded in a paraffin moderator, surrounded by a Cd layer and additional paraffin shielding. The ion beam from the mass spectrometer is stopped on a catcher, which is located in the center of the  $^3\text{He}$  counter array and faces a 51 mm diam  $\times$  0.3 mm NE 102A plastic scintillator.

From the simultaneous multiscaling of the  $\beta$  and the neutron activity, information on the half-lives of the Li and Na isotopes and their decay daughters

can be deduced, and the delayed neutron emission probability  $P_n$  can be determined from the ratio of both activities. Furthermore, the delayed emission of two neutrons can be identified by demanding twofold coincidences between any two of the eight  $^3\text{He}$  counters.

### C. $\beta$ telescope

$\beta$  spectra were taken by a scintillator telescope<sup>17</sup> consisting of a 0.5 mm thick NE 102A detector and a 5 cm diam  $\times$  10 cm NE 102A detector. The linearity of the detector response has been verified

with monoenergetic electrons from the Heidelberg betatron.

### D. $\beta$ - $\gamma$ detection setup

Despite the distance from the target (6 m) and the heavy shielding (0.6 m iron and 1.6 m concrete), the residual flux of fast neutrons ( $250 \text{ n cm}^{-2} \text{ sec}^{-1}$ ) was too high to allow the use of a Ge(Li) detector which would have been damaged within a few hours.

Therefore, for  $\gamma$  detection a 76 mm diam  $\times$  76 mm NaI(Tl) scintillator was mounted close to the

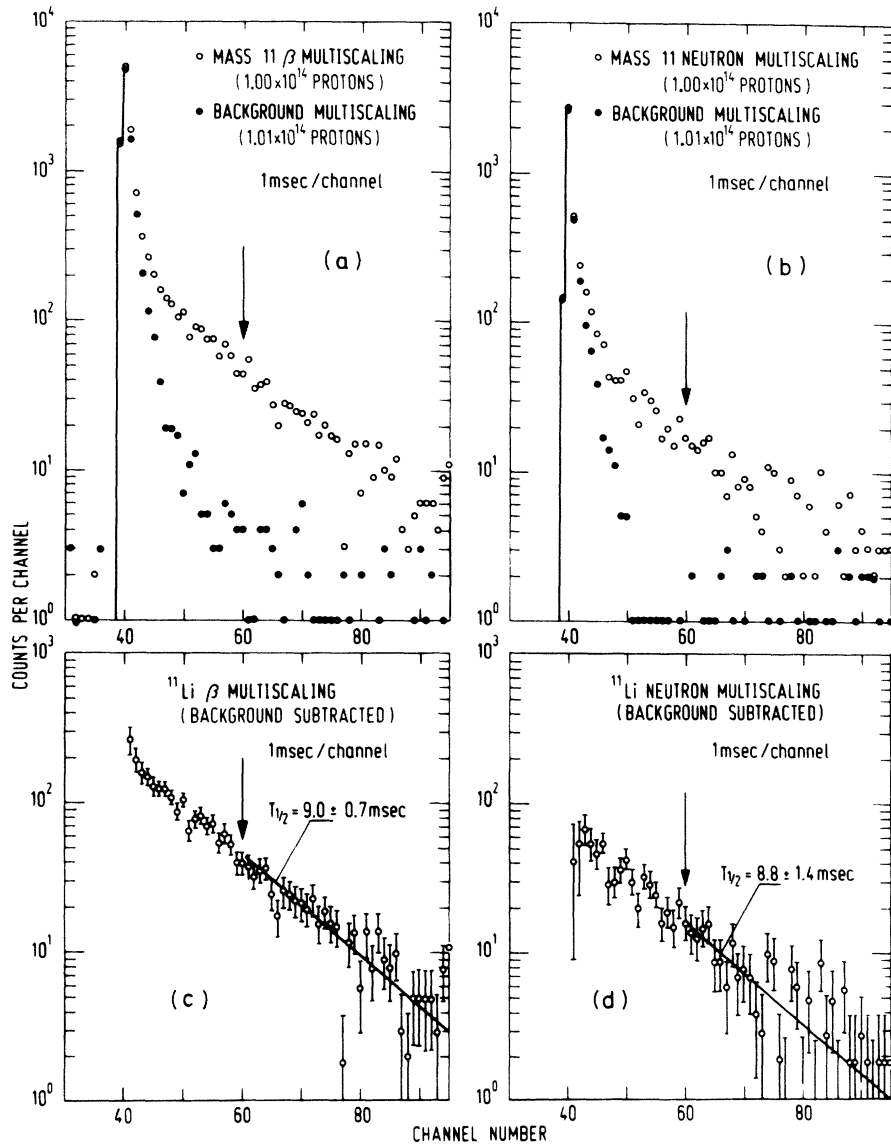


FIG. 1.  $\beta$  and neutron multiscaling curves for  $^{11}\text{Li}$ . In (a) and (b) the raw data are shown as obtained from a time analysis of the  $\beta$  and neutron activity at mass 11 together with a background run. In (c) and (d) the net effects are plotted after background subtraction. The proton beam occurs at channel 39. The arrows indicate the time of switching off the ion beam. The results of least-squares fits for the  $^{11}\text{Li}$  half-life are also given.

catcher foil at  $90^\circ$  with respect to the ion beam direction. A 51 mm diam  $\times 0.3$  mm NE 102A plastic scintillator, facing the catcher foil, was used for  $\beta$  detection. Maximum efficiency was searched for by optimizing the solid angles under which the two detectors were seen from the ion collecting foil.

Discrimination against the rather intense  $\gamma$  background was obtained by selecting  $\gamma$  rays in coincidence with  $\beta$  particles within a 200 nsec time window. The  $\beta$  coincident  $\gamma$  spectra were stored in different parts of the multichannel memory during four consecutive time intervals after the proton burst. Simultaneously with the storage of the  $\gamma$  spectra, the  $\beta$  singles rate was counted in a multiscaling mode, thereby enabling the determination of the absolute  $\gamma$  ray intensities per  $\beta$  decay.

### 3. MEASUREMENTS AND RESULTS

#### A. Half-lives

Three independent methods were applied for the half-life determination. The first two are multiscaling of the  $\beta$  and the neutron activities as a function of time. Examples for the results at mass

11 and 29 are shown in Figs. 1 and 2, respectively. For the low cross section isotopes, background runs were carried out under identical timing conditions, but with the ion beam switched off, and for the same integral number of protons. The third method is ion counting during the diffusion process, with a triangular modulation of the acceleration potential.<sup>2,4,5</sup>

In Table I the results of half-life measurements for  $^9,^{11}\text{Li}$ ,  $^{27-33}\text{Na}$ , and  $^{29,30}\text{Mg}$  are shown. Clearly ion counting is the most accurate and sensitive method. The good agreement with the results obtained from the activity measurements confirms the validity of the underlying assumption of mass-independent diffusion characteristics. Activity multiscaling, on the other hand, offers the advantage of additionally revealing the decay properties of the radioactive daughters. Thereby the half-life of  $^{29}\text{Mg}$  could be determined (see Fig. 2) to be  $1470 \pm 90$  msec in slight disagreement with the recent result of  $1200 \pm 130$  msec obtained by Goosman, Davids, and Alburger.<sup>14</sup> From its  $\beta$  activity a half-life of  $1200 \pm 500$  msec was ascribed to the new isotope  $^{30}\text{Mg}$ .

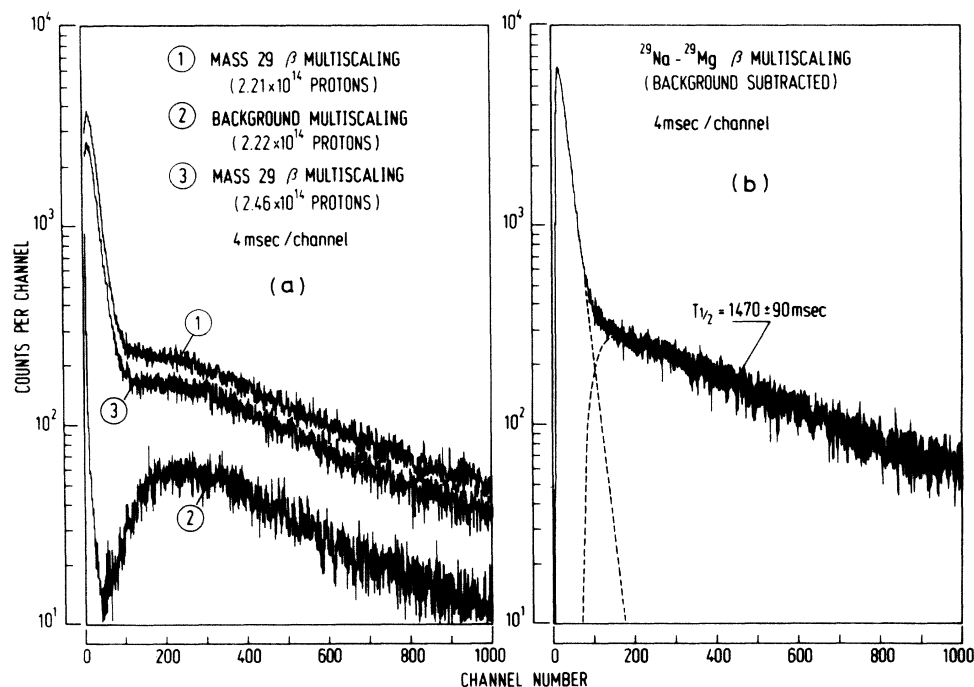
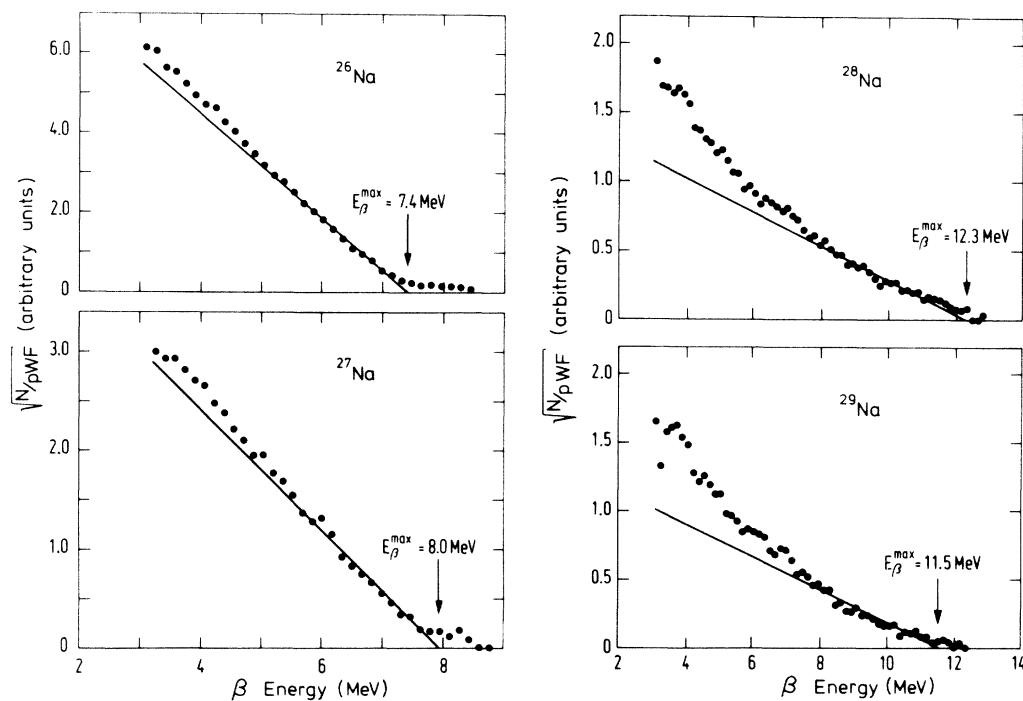


FIG. 2.  $\beta$  multiscaling curve for  $^{29}\text{Na}$ ,  $^{29}\text{Mg}$ . In (a), the results of two separate runs (curves 1 and 3) are shown together with an intermediate background measurement (curve 2). The broad peak in the background spectrum is tentatively ascribed to  $\beta$ -active neutral particulates produced by the proton bombardment of the heated uranium-graphite target. The position of the intensity maximum is interpreted as the average time of flight of these products between target and catcher. The proton beam occurs at channel 5. In (b) the net result after background subtraction is plotted. Since no ion beam deflector was used the short lived component contains both the diffusion and the decay properties of  $^{29}\text{Na}$ . The result of a least-squares fit for the decay of the daughter isotope  $^{29}\text{Mg}$  is given.

FIG. 3.  $\beta$  spectra of  $^{26-29}\text{Na}$ .B.  $P_n$  values

The delayed neutron emission probability  $P_n$  is the ratio of the simultaneously detected  $\beta$  and neutron activity. For a direct  $P_n$  determination the ratio of detection efficiencies for the counters has to be known. The known  $P_n$  value of  $^9\text{Li}$  was used to determine the efficiency ratio *in situ*. Assuming that the delayed neutron from the other precursors have predominantly low energy (which is the case

for all measured spectra), similar to  $^9\text{Li}$ , we used this efficiency calibration to extract the  $P_n$  for all cases. The  $P_n$  value of  $^9\text{Li}$  as measured by Chen, Tombrello, and Kavanagh<sup>18</sup> to be  $35.0 \pm 3.5\%$  was preferred for this calibration against the older value<sup>19</sup> of  $75 \pm 15\%$ . This assumption is supported by  $P_n$  measurements for Rb and Cs isotopes based on the same calibration procedure, which are found<sup>20</sup> to be in fair agreement with a variety of  $P_n$  values obtained by other authors. The results

TABLE I. Half-life measurements (msec).

Nucleus	$\beta$ counting	Neutron counting	Ion counting <sup>a</sup>	Best value	Other work
$^9\text{Li}$	$179 \pm 8$	$175 \pm 1$		$175 \pm 1$	$177 \pm 3$ <sup>b</sup>
$^{11}\text{Li}$	$9.0 \pm 0.8$	$8.8 \pm 1.4$	$8.5 \pm 0.2$	$8.5 \pm 0.2$	
$^{27}\text{Na}$	$308 \pm 7$	$370 \pm 110$	$295 \pm 10$	$304 \pm 7$	$280 \pm 20$ <sup>c</sup>
$^{28}\text{Na}$	$30.2 \pm 0.4$	$26 \pm 5$	$32.0 \pm 0.8$	$30.5 \pm 0.4$	
$^{29}\text{Na}$	$40.8 \pm 7.0$	$40.6 \pm 2.3$	$44.0 \pm 1.5$	$42.9 \pm 1.5$	
$^{30}\text{Na}$	$54 \pm 12$	$52.2 \pm 3.6$	$53.5 \pm 3.0$	$53.0 \pm 3.0$	
$^{31}\text{Na}$	$21 \pm 3$	$20 \pm 5$	$16.6 \pm 0.7$	$16.9 \pm 0.7$	
$^{32}\text{Na}$			$13.5 \pm 1.5$	$13.5 \pm 1.5$	
$^{33}\text{Na}$			$20 \pm 15$	$20 \pm 15$	
$^{29}\text{Mg}$	$1470 \pm 90$			$1470 \pm 90$	$1200 \pm 130$ <sup>d</sup>
$^{30}\text{Mg}$	$1200 \pm 500$			$1200 \pm 500$	

<sup>a</sup> This work, previous work (Ref. 2), and R. Klapisch in CERN Report No. CERN 70-30, 1970 (unpublished), p. 21.

<sup>b</sup> See Ref. 18.

<sup>c</sup> See Ref. 22.

<sup>d</sup> See Ref. 14.

TABLE II.  $P_n$  values.

Precursor	$P_n$ value <sup>a</sup> (%)
<sup>9</sup> Li	(35.0 ± 3.5)
<sup>11</sup> Li	60.8 ± 7.2
<sup>27</sup> Na	0.08 ± 0.03
<sup>28</sup> Na	0.58 ± 0.12
<sup>29</sup> Na	15.1 ± 1.8
<sup>30</sup> Na	33.1 ± 3.8
<sup>31</sup> Na	30 ± 8

<sup>a</sup> Normalized for  $P_n(^9\text{Li}) = 35.0\%$  (Ref. 18).

are compiled in Table II. No evidence for the  $\beta$  delayed double neutron emission could be deduced from neutron-neutron coincidences carried out for <sup>11</sup>Li and <sup>29-31</sup>Na, due to the high random-coincidence contribution.

It is worth noting that only five light delayed neutron emitters had been reported before this work.<sup>21</sup> Furthermore, the  $P_n$  data for the isotopes <sup>27-31</sup>Na represent the first case where a systematic variation of  $P_n$  with the neutron number has been studied for light nuclei. A simple semiempirical description based on the concept of  $\beta$  strength function, which seems to be applicable to heavier delayed neutron emitters,<sup>20</sup> cannot account for the experimental  $P_n$  values of the Na isotopes.

#### C. Maximum $\beta$ energies

Figure 3 shows Fermi-Kurie plots of the  $\beta$  spectra of <sup>26-29</sup>Na taken with the  $\beta$  telescope. The energy calibration during the on-line measurements was achieved by introducing sources of <sup>207</sup>Bi, <sup>60</sup>Co, and <sup>228</sup>Th. The stability of this calibration was checked by recording the  $\beta$  spectrum of <sup>26</sup>Na at regular intervals.

The deduced  $\beta$  end-point energies  $E_\beta$  and  $Q_\beta$  values are compiled in Table III and compared with other works. Our end-point energies for <sup>26</sup>Na and <sup>27</sup>Na agree with the results from previous decay studies.<sup>13,22</sup> Since there are dominant  $\beta$  branches in the decays of <sup>26</sup>Na and <sup>27</sup>Na to known excited levels (see Sec. 4 A and Refs. 22, 23, and 24), the  $Q_\beta$  values can be safely deduced from the end points of the singles  $\beta$  spectra in these cases.

For <sup>28</sup>Na and <sup>29</sup>Na one cannot readily extract a value of  $Q_\beta$ . There are  $\beta$  branches to the ground state as well as to different excited states in the Mg daughter nuclei (see Secs. 4 B and 4 C). In the case of <sup>29</sup>Na there is even a 15%  $\beta$  decay branch (see Table II) to excited states above the <sup>29</sup>Mg neutron binding energy of 3.645 MeV.<sup>14,25</sup>

A decomposition of the Fermi-Kurie plot into different components was not undertaken in view of the much more precise  $Q_\beta$  values, which can be obtained from the recent data for the ground state masses of Na and Mg isotopes (compare Table III).

#### D. $\gamma$ rays from <sup>27-29</sup>Na decay

A systematic investigation of the  $\gamma$  spectra from the decay of the isotopes <sup>25-29</sup>Na was carried out, with background measurements (ion beam switched off) interspersed among the regular runs.

In Fig. 4 the  $\beta$ -coincident  $\gamma$  spectrum from the decay of <sup>29</sup>Na is shown. The absolute calibration of the efficiency of the  $\beta$ - $\gamma$  detector system was obtained *in situ* from the known  $\gamma$  activities of <sup>25</sup>Na<sup>23</sup> and <sup>26</sup>Na.<sup>22,24</sup> Figure 5 shows the variation of this efficiency with the  $\gamma$  energy. The deduced absolute  $\gamma$  intensities per  $\beta$  decay are based upon this calibration, which introduces an over-all uncertainty of 20%. The  $\gamma$  lines and intensities ascribed to the decays of <sup>27-29</sup>Na are compiled in Table IV.

TABLE III.  $Q_\beta$  value measurements.

Decay	This work		Previous decay work	
	$E_\beta^{\text{max}}$ (keV)	Deduced $Q_\beta^a$ (keV)	$Q_\beta$ (keV)	$Q_\beta$ (keV) from mass measurements <sup>b</sup>
<sup>26</sup> Na	7400 ± 400	9200 ± 400	9000 ± 500 <sup>c</sup> 9209 ± 200 <sup>d</sup>	9310 ± 15
<sup>27</sup> Na	8000 ± 500	9000 ± 500	8600 ± 500 <sup>c</sup> 8935 ± 180 <sup>d</sup>	8970 ± 60
<sup>28</sup> Na	12 300 ± 700	≥ 12 300		13 880 ± 85
<sup>29</sup> Na	11 500 ± 800	≥ 11 500		13 240 ± 95

<sup>a</sup> The  $Q_\beta$  values are deduced from  $E_\beta^{\text{max}}$  as described in the text.

<sup>b</sup>  $Q_\beta$  values deduced from the experimental ground state mass excesses of <sup>26-29</sup>Na (Ref. 12), <sup>26</sup>Na [from E. R. Flynn and J. D. Garrett, Phys. Rev. C **9**, 210 (1974)], <sup>26-28</sup>Mg (Ref. 25), and <sup>29</sup>Mg (Ref. 14).

<sup>c</sup> See Ref. 13.

<sup>d</sup> See Ref. 22.

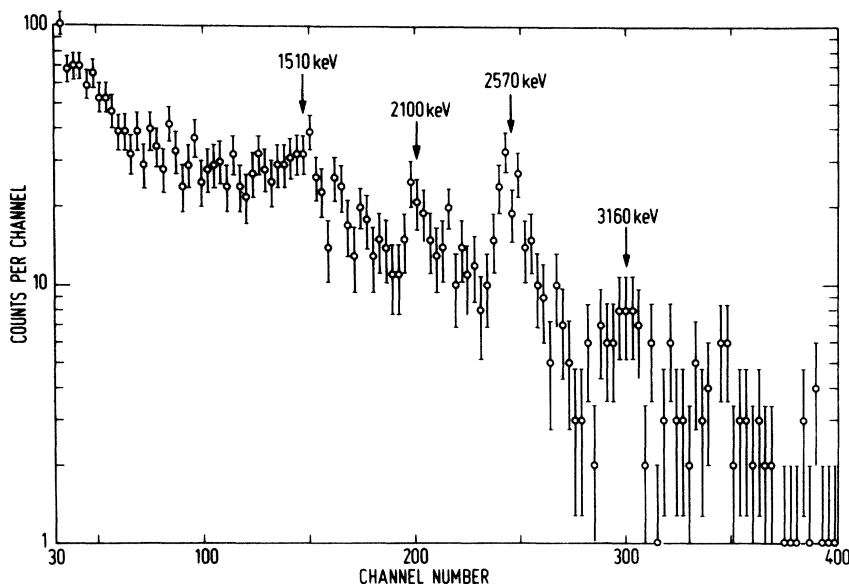


FIG. 4.  $\gamma$  spectrum from the decay of  $^{29}\text{Na}$ , obtained from  $2.2 \times 10^{14}$  protons and counting intervals of 10–110 msec after the proton pulse. The corresponding  $\beta$  multiscaling curves obtained simultaneously are shown in Fig. 2.

4. DISCUSSION

A.  $^{27}\text{Na}$  decay

While this work was in progress, Alburger, Goosman, and Davids<sup>22</sup> reported the  $\beta$  decay scheme of  $^{27}\text{Na}$ . The present results confirm the occurrence of two prominent  $\gamma$  rays with energies of 985 and 1698 keV. For the sum of their absolute intensities we found  $131 \pm 26\%$  (see Table IV). This is consistent with the assumption that 100% of the  $\beta$  decay of  $^{27}\text{Na}$  populates either the 984.7 keV ( $\frac{3}{2}^+$ ) or the 1698.7 keV ( $\frac{5}{2}^+$ ) level of  $^{27}\text{Mg}$ . No other  $\gamma$  rays were observed although several could have been expected from possible allowed  $\beta$  decays. A  $J^\pi = \frac{3}{2}^+$  or  $\frac{5}{2}^+$  assignment for  $^{27}\text{Na}$  results from the allowed character of the two observed  $\beta$  branches.

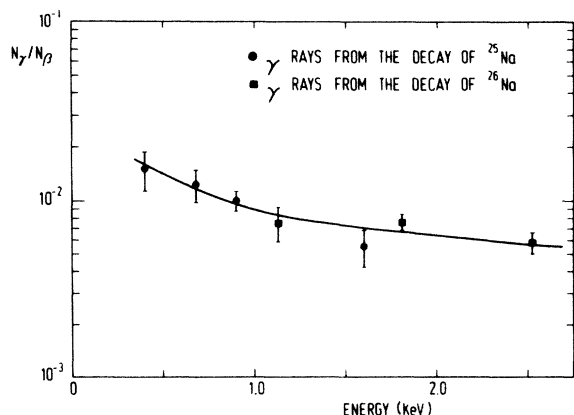


FIG. 5. Calibration for the  $\beta$ - $\gamma$  detector array.

In Table V the branching ratios obtained (normalized to a sum of 100%), upper limits for some unobserved  $\beta$  branches, and  $\log ft$  values are compared with results from previous work.

B.  $^{28}\text{Na}$  decay

Two  $\gamma$  rays are observed in the  $\beta$  coincident  $\gamma$  spectrum taken at mass 28. They are found to decay with a half-life compatible with the known half-life of  $^{28}\text{Na}$ . Their energies and intensities are listed in Table IV. These  $\gamma$  energies can be matched with the known  $^{28}\text{Mg}$  levels<sup>25</sup> (Fig. 6) by assuming that the first  $\gamma$  ray corresponds to the

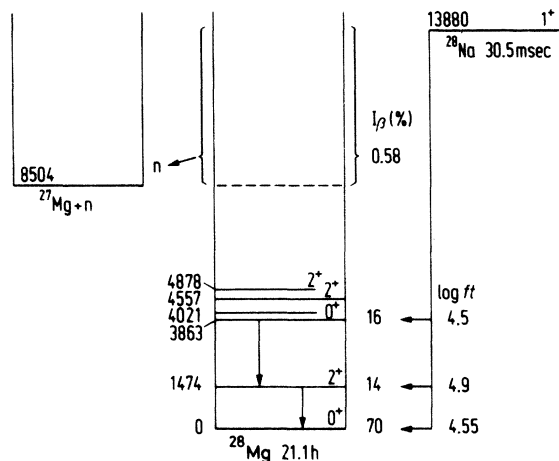


FIG. 6. Decay scheme of  $^{28}\text{Na}$ .

TABLE IV.  $\gamma$  ray energies and intensities from the decay of  $^{27-29}\text{Na}$ .

Parent nucleus	$\gamma$ ray energy (keV)	$\gamma$ ray intensity (%)
$^{27}\text{Na}$	$985 \pm 15$	$117 \pm 25$
	$1698 \pm 15$	$14 \pm 3$
$^{28}\text{Na}$	$1475 \pm 15$	$30 \pm 5$
	$2380 \pm 20$	$16 \pm 3$
$^{29}\text{Na}$	$1510 \pm 20$	$7 \pm 2$
	$2100 \pm 25$	$4.5 \pm 2.0$
	$2570 \pm 30$	$12.5 \pm 2.0$
	$3160 \pm 40$	$3.0 \pm 1.5$

decay of the excited  $2^+$  state at 1473.5 keV and the second to the decay of the excited  $0^+$  state at 3862.7 keV to the 1473.5 keV  $2^+$  state. None of the possible  $\gamma$  rays from the two excited  $2^+$  states at 4557.3 and 4878.1 keV were observed with intensities above 10%. If one assumes that the only  $\gamma$  feeding to the 1473.5 keV  $2^+$  state is the observed  $\gamma$  ray from the 3862.7 keV  $0^+$  state, then the  $\beta$  branching to the  $2^+$  level of  $^{28}\text{Mg}$  can be calculated as the difference between the  $\gamma$  intensities from and to this level, which is  $14 \pm 6\%$ . The occurrence of allowed  $\beta$  decays to a  $2^+$  and a  $0^+$  state leads to a  $1^+$  assignment for  $^{28}\text{Na}$ . Therefore, the 70% of the  $\beta$  decay which is yet unaccounted for could be assumed to feed the  $^{28}\text{Mg}$   $0^+$  ground state through an allowed decay. Since the statistics of the  $^{28}\text{Na}$   $\beta$  spectrum (Fig. 3) did not allow a decomposition, no direct experimental evidence for the ground state  $\beta$  branch could be shown by means of the experimental techniques used in this work.

### C. $^{29}\text{Na}$ decay

Four  $\gamma$  lines (see Table IV) are apparent from the  $^{29}\text{Na}$   $\gamma$  spectrum of Fig. 4. Even if no cascade is involved these  $\gamma$  rays account for only  $27 \pm 6\%$  of the  $\beta$  decay of  $^{29}\text{Na}$ . In the same way as for the  $^{28}\text{Na}$  decay, it can be assumed that the portion of  $\beta$  activity with which we do not record coincident  $\gamma$  rays or neutrons, corresponds to a  $\beta$  decay to the  $^{29}\text{Mg}$  ground state with a branching ratio of about 58%.

Since the level scheme of  $^{29}\text{Mg}$  is unknown, the  $\gamma$  rays cannot be assigned to transitions between  $^{29}\text{Mg}$  states. However, one possible assignment should be mentioned. The  $1510 \pm 20$  keV ( $7 \pm 2\%$ )  $\gamma$  ray could correspond to the  $\gamma$  decay of the  $2^+$  state of  $^{28}\text{Mg}$ , subsequent to a delayed neutron emission to this excited state rather than to the  $^{28}\text{Mg}$  ground state. According to the  $P_n$  value of

TABLE V.  $^{27}\text{Na}$   $\beta$  decay.

$^{27}\text{Mg}$ level <sup>a</sup> $E_{\text{exc}}$ (keV)	$J^\pi$	This work <sup>b</sup>		Previous work <sup>c</sup>	
		$\beta$ (%)	$\log ft$	$\beta$ (%)	$\log ft$
984.7	$\frac{3}{2}^+$	89	4.05	86	4.1
1698.3	$\frac{5}{2}^+$	11	4.7	14	4.7
1939.9	$\frac{5}{2}^+$	<1.3	>5.7	<3.5	>5.3
3109.2	$(\frac{3}{2}^+, \frac{7}{2}^+)$	<0.6	>5.7	<2.9	>5.0
3476.1	$\frac{1}{2}^+$	<1.1	>5.25	<2.0	>5.0

<sup>a</sup> See Ref. 25.

<sup>b</sup> The  $\beta$  intensity is calculated from the absolute  $\gamma$  intensity by use of the decay scheme of  $^{27}\text{Mg}$  from G. Costa and F. A. Beck, Nucl. Phys. **A181**, 132 (1972). The  $\log ft$  values are calculated from the graphs compiled by C. M. Lederer, J. M. Hollander, and I. Perlman, *Table of Isotopes* (Wiley, New York, 1967), 6th ed.

<sup>c</sup> See Ref. 22.

$15.1 \pm 1.8\%$  this decay mode would account for about half of the total delayed neutron branch. However, this assignment is unlikely in view of the apparent incompatibility of the measured  $\gamma$  energy with the expected value of 1473.5 keV. Here, clearly, the impossibility of using a Ge(Li) detector was detrimental. A search for corresponding structures in the delayed neutron spectrum of  $^{29}\text{Na}$  by means of a  $^3\text{He}$  spectrometer failed because of lack of statistics.

### CONCLUSION

Although the knowledge about light neutron rich nuclei is rapidly increasing, no information on excited states was available before, for the decay of nuclei past  $T_x = \frac{5}{2}$  ( $^{27}\text{Na}$ ). This work demonstrates the possibility of obtaining spectroscopic information for nuclei that are considerably further from stability. In the case of the lithium and sodium isotopes to which our technique applies, further progress depends critically on an increase in the intensities of the separated short-lived isotopes. It is also necessary to use still better shielding that would allow the use of Ge(Li) detectors. This seems within reach in the near future, resulting in better  $\gamma$  spectra for the isotopes to  $^{29}\text{Na}$  and possibly data for the more distant  $^{30}\text{Na}$  and  $^{31}\text{Na}$ .

As we reach the vicinity of the neutron drip line, delayed neutron emission is going to be a very general and even predominant mode of decay. Some light nuclei in this region will in fact have few if any bound excited states. Delayed neutron branching ratios (and energy spectra if they could be measured) are then very precious spectroscopic information.

## ACKNOWLEDGMENTS

We are indebted to Arthur M. Poskanzer for stimulating discussions and for the many valuable suggestions he made while he was participating in a companion experiment. It is a pleasure to acknowledge the excellent contributions of R. Ferg-

eau, M. Jacotin, and J. F. Kepinski who built the mass spectrometer and related equipment and assisted during the run at CERN. We are grateful to Alan Ball and all the members of the CERN heavy liquid bubble chamber group, whose help was essential in installing the experiment and maintaining the complex beam transport.

\*Gesellschaft für Schwerionenforschung mbH, Darmstadt, Germany.

†Alexander von Humboldt Fellow 1972–73 at the Institut für Kernchemie, Universität Mainz, on foreign assignment from Oak Ridge National Laboratory operated by Union Carbide Corporation under contract with the U.S. Atomic Energy Commission.

‡Institut de Physique Nucléaire, Orsay, France.

<sup>1</sup>J. D. Bowman, A. M. Poskanzer, R. G. Korteling, and G. W. Butler, *Phys. Rev. Lett.* **31**, 614 (1973).

<sup>2</sup>R. Klapisch, C. Thibault, A. M. Poskanzer, R. Prieels, C. Rigaud, and E. Roeckl, *Phys. Rev. Lett.* **29**, 1254 (1972).

<sup>3</sup>V. V. Volkov, in *Proceedings of the International Conference on Nuclear Physics, Munich, Germany, 1973*, edited by J. de Boer and H. J. Mang (North-Holland, Amsterdam/American Elsevier, New York, 1974), Vol. 2, p. 279.

<sup>4</sup>C. Thibault, Ph.D. thesis, Faculté des Sciences, Orsay, 1971 (unpublished).

<sup>5</sup>C. Rigaud, Thèse de 3e cycle, Faculté des Sciences, Orsay, 1972 (unpublished).

<sup>6</sup>G. W. Butler, A. M. Poskanzer, and D. A. Landis, *Nucl. Instrum. Methods* **89**, 189 (1970); J. D. Bowman, A. M. Poskanzer, R. G. Korteling, and G. W. Butler, *Phys. Rev. C* **9**, 836 (1974).

<sup>7</sup>J. C. Jacmart, M. Liu, F. Mazloum, M. Riou, J. C. Roynette, and C. Stephan, *Rev. Phys. Appl.* **4**, 99 (1969).

<sup>8</sup>A. G. Artukh, V. V. Avdeichikov, J. E. Erö, G. F. Gridnev, V. L. Mikheev, and V. V. Volkov, *Nucl. Instrum. Methods* **83**, 72 (1970).

<sup>9</sup>A. G. Artukh, V. V. Avdeichikov, G. F. Gridnev, V. L. Mikheev, V. V. Volkov, and J. Wilczynski, *Nucl. Phys.*

*A176*, 284 (1971).

<sup>10</sup>A. G. Artukh, G. F. Gridnev, V. L. Mikheev, V. V. Volkov, and J. Wilczynski, *Nucl. Phys.* **A192**, 170 (1972).

<sup>11</sup>R. Klapisch, R. Prieels, C. Thibault, A. M. Poskanzer, C. Rigaud, and E. Roeckl, *Phys. Rev. Lett.* **31**, 118 (1973).

<sup>12</sup>C. Thibault, R. Klapisch, C. Rigaud, A. M. Poskanzer, L. Lessard, and W. Reisdorf, to be published.

<sup>13</sup>R. Klapisch, C. Thibault-Philippe, C. Détraz, J. Chaumont, R. Bernas, and E. Beck, *Phys. Rev. Lett.* **23**, 652 (1969).

<sup>14</sup>D. R. Goosman, C. N. Davids, and D. E. Alburger, *Phys. Rev. C* **8**, 1331 (1973).

<sup>15</sup>Preliminary results of this work were presented, in *Proceedings of the International Conference on Nuclear Physics, Munich, Germany, 1973*, edited by J. de Boer and H. J. Mang (See Ref. 3), Vol. 1, p. 326.

<sup>16</sup>E. Roeckl and P. F. Dittner, to be published.

<sup>17</sup>E. Beck, *Nucl. Instrum. Methods* **76**, 77 (1969).

<sup>18</sup>Y. S. Chen, T. A. Tombrello, and R. W. Kavanagh, *Nucl. Phys.* **A146**, 136 (1970).

<sup>19</sup>D. E. Alburger, *Phys. Rev.* **132**, 328 (1963).

<sup>20</sup>E. Roeckl, P. F. Dittner, R. Klapisch, C. Thibault, C. Rigaud, and R. Prieels, *Nucl. Phys.* **A222**, 621 (1974).

<sup>21</sup>P. del Marmol, *Nucl. Data* **A6**, 141 (1969).

<sup>22</sup>D. E. Alburger, D. R. Goosman, and C. N. Davids, *Phys. Rev. C* **8**, 1011 (1973).

<sup>23</sup>D. E. Alburger and D. H. Wilkinson, *Phys. Rev. C* **3**, 1957 (1971).

<sup>24</sup>G. Klotz, J. P. Gonidec, P. Baumann, and G. Walter, *Nucl. Phys.* **A205**, 90 (1973).

<sup>25</sup>P. M. Endt and C. Van der Leun, *Nucl. Phys.* **A214**, 1 (1973).